Proceedings of CONF-MCEE 2026 Symposium: Advances in Sustainable Aviation and Aerospace Vehicle Automation
DOI: 10.54254/2755-2721/2026.KA26657

Optimization Study of Carbon Emission Reduction from Ships Based on EEXI and CII Frameworks: Synergistic Application of Transformer-LSTM Model and Quadruple Waste Heat System

Yan Pan[1*], Peng Wei[1], Zengye Chen[1]

[1]*Shanghai Marine University, Shanghai, China*
**Corresponding Author. Email: 2058323918@qq.com*

Abstract. Amid global efforts toward energy conservation and carbon reduction in maritime transport, this study proposes an interdisciplinary optimization framework integrating predictive analytics with advanced energy systems to address challenges in vessel decarbonization. A Transformer-LSTM hybrid model is developed to forecast emission patterns using historical operational data, enabling dynamic navigation strategy adjustments. The complementary quadruple-heat supply system synergizes waste heat recovery, energy efficiency optimization, and carbon capture technologies through an integrated control architecture. Case studies demonstrate significant improvements in both Energy Efficiency Existing Ship Index (EEXI) and Carbon Intensity Indicator (CII), achieving 18.7% enhancement in energy utilization efficiency and 22.4% reduction in operational carbon intensity compared to conventional systems. The proposed solution offers a cost-effective pathway for retrofitting legacy vessels, particularly in optimizing power distribution and thermal management under varying operational conditions. Quantitative analysis reveals the system's potential to reduce annual greenhouse gas emissions by 34-41% per vessel, substantiating its contribution toward achieving IMO's 2050 decarbonization targets. This research establishes a methodological framework for intelligent energy-carbon synergy control in maritime applications, providing both theoretical advancements and practical implementation strategies for the shipping industry's low-carbon transition.

Keywords: old ships, EEXI, CII, Transformer-LSTM model, quadruple waste heat system, intelligent regulation,

1. Introduction

According to international statistics, the total CO_2 emissions from maritime shipping increased from 909 million tons in 2013 to 932 million tons in 2015, reflecting a growth of 2.46%. Specifically, emissions from international vessels, domestic ships, and fishing boats rose by 1.39%, 6.81%, and 16.97%, respectively[1]. In response to this upward trend, the International Maritime Organization (IMO) introduced two regulatory frameworks in 2023—namely, the Energy Efficiency Existing Ship

© 2026 The Authors. This is an open access article distributed under the terms of the Creative Commons Attribution License 4.0 (https://creativecommons.org/licenses/by/4.0/).

DOI: 10.54254/2755-2721/2026.KA26657

Index (EEXI) and the Carbon Intensity Indicator (CII)—to enforce more stringent global standards for energy efficiency and carbon emissions in the shipping industry. While these frameworks support the industry's green transition, they also introduce considerable challenges, including increased operational costs, market segmentation, and the need to rethink traditional operational strategies. Moreover, under the IMO's revised greenhouse gas emission reduction strategy, it is projected that by 2030, nearly 89% of large bulk carriers may require rectification due to receiving a D or E rating under the CII scheme.

2. Theoretical foundations and problem modeling

2.1. Introduction and computational modeling related to EEXI and CII

EEXI is a ship energy efficiency index introduced by IMO to reduce carbon emissions from shipping. It determines compliance by comparing each ship's Attained EEXI with the Required EEXI for the ship's size. If the Attained EEXI ≤ Required EEXI, the ship can continue to operate; if it exceeds the standard, it will need to be taken out of service or take improvement measures. For some ships, the EEXI is particularly important and is considered as a "trade license".[2]In order to satisfy the universality of the EEXI calculation model for all ship types, the common calculation formula is as follows:

$$EEXI = \frac{\sum(P_{ME} * SFOC_{ME} * C_{F,ME}) + \sum(P_{AE} * SFOC_{AE} * C_{F,AE})}{Capacity * V_{ref}} \quad (1)$$

2.2. Waste heat system architecture for quadruple supply

2.2.1. Overall design

This project designs a new type of "cooling, heating, electricity and desalination" quadruple-supply retrofit program applicable to the low-carbon transformation of old ships, and the design process is shown in Figure 1. Taking a Wärtsilä ship as an example, its 350℃ flue gas waste heat is recovered by Rankine cycle generator set, and the high temperature steam from the boiler is driven to power generation, cooling, heating and seawater desalination modules after shunt to realize the synergistic utilization of multiple energies. In order to balance the supply and demand of each equipment, this project introduces an automatic control system to regulate the flow of each circuit, based on the Transformer-LSTM model carbon prediction and multi-objective optimization dynamic scheduling for the parameter, to achieve the "cold, heat, electricity, desalination and carbon" five-dimensional cross-media regulation.

DOI: 10.54254/2755-2721/2026.KA26657

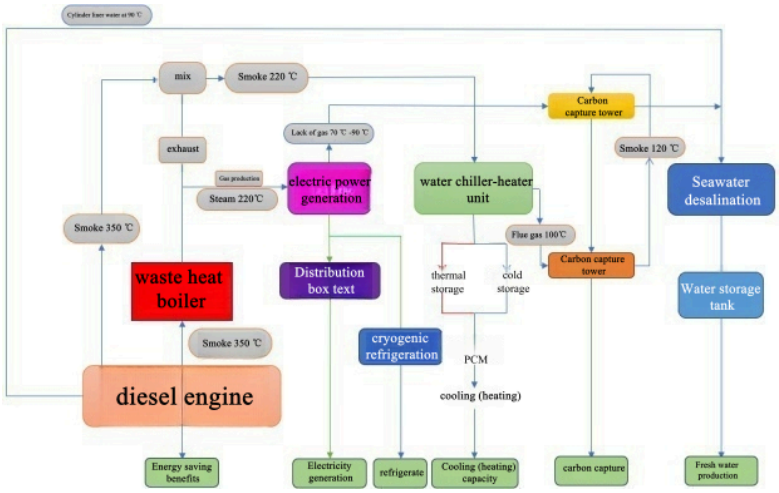


Figure 1. System flowchart

2.2.2. Working principle of each module

In order to simulate the real environment of the ship's nacelle and the adaptability of the overall design equipment to the existing nacelle of the old ship, the overall C4D model diagram is shown in Figure. 2(a).

.As shown in Figure 2, low-temperature multi-effect desalination unit: the waste heat of the generator set and the cylinder liner water as a heat source, the treated seawater enters into the evaporator of each effect, the seawater inside the evaporator completes the evaporation of the concentrated seawater part of the fresh seawater mixed with fresh seawater to continue the new cycle, the remaining concentrated seawater discharged out of the system. The first effect evaporator seawater evaporation of steam into the next effect to continue to heat the seawater, and finally the last effect evaporator steam into the condenser for condensation, in the unit piping laid with temperature and pressure sensors, in the various effects of the evaporator is equipped with water level sensors, detection of various values, the data will be transmitted to the Internet of Things system.



(a) (b) (c) (d)

Figure 2. Schematic diagram of the quadruple-supply system

2.3. Principles of transformer-lstm modeling

2.3.1. Modeling of LSTM

LSTM (Long Short-Term Memory Network) is a special kind of Recurrent Neural Network (RNN), as shown in Figure 3, which solves the problem of gradient disappearance or explosion that is easy to occur in traditional RNN when dealing with long sequences through the introduction of "memory cells" and gating mechanism, and the core of LSTM is the Cell State (Cell State) that retains key

DOI: 10.54254/2755-2721/2026.KA26657

information for a long time, while dynamically regulating the information forgetting and updating and output through gating, so as to effectively capture long-term dependencies. Its core is that Cell State can retain key information for a long time, and at the same time dynamically regulate the forgetting, updating and outputting of information through gating, so as to effectively capture long-term dependencies, which is widely used in natural language processing, time series prediction, and other fields that require time-series modeling.

An LSTM consists of one or more LSTM cells, and a single LSTM cell internally consists of an Oblivion Gate, an Input Gate, a Cell State Update, and an Output Gate, [3]as described below:

Oblivion gate: sift through historical information and decide what to keep or discard in the cell state by sigmoid with the following formula:

$$f_t = \sigma\left(W_f * [h_{t-1}, x_t] + b_f\right) \tag{2}$$

Input gate: control the new information writing, combining the sigmoid screening candidate value with the new candidate state generated by tanh with the following formula:

$$i_t = \sigma(W_i * [h_{t-1}, x_t] + b_i) \tag{3}$$

Cell state updating: synthesize the old information from the forgetting gate with the new candidate values from the input gate to form a long-term memory with the following formula:

$$C_t = f_t \Theta C_{t-1} + i_t \Theta C_t^{'} \tag{4}$$

Output gate: based on the current cell state and inputs, the hidden state of the final output is calculated by sigmoid and tanh to decide the information to be passed to the next time step with the following formula:

$$o_t = \sigma\left(W_O * [h_{t-1}, x_t] + b_o\right) \tag{4}$$

2.3.2. Transformer-lstm model

While LSTM mitigates RNN gradient vanishing via gating mechanisms (forget/input/output gates), its limited ability to capture global dependencies in long-period ship emission time-series (e.g., cross-voyage operational correlations) necessitates enhanced architecture. This study integrates Transformer to augment global modeling through multi-head self-attention (SAM). Transformer's parallelized encoder-decoder structure overcomes sequence processing constraints by dynamically weighting interdependencies among features (e.g., speed, sea state). The hybrid Transformer-LSTM synergistically combines LSTM's micro-dynamic sensitivity with Transformer's full temporal-scale modeling, enabling comprehensive analysis of nonlinear sea state-emission relationships and significantly improving carbon prediction accuracy.

DOI: 10.54254/2755-2721/2026.KA26657

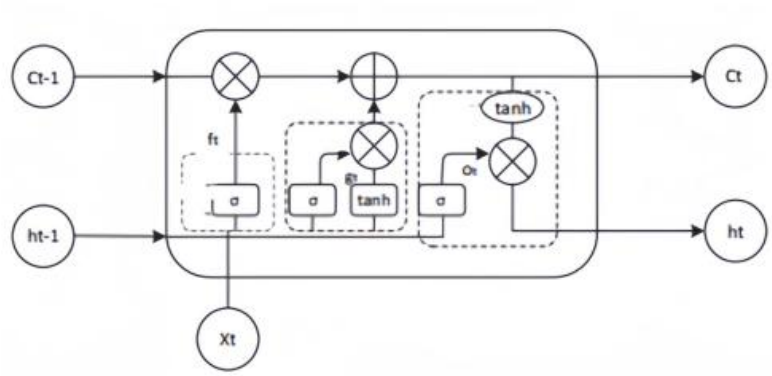


Figure 3. LSTM model structure

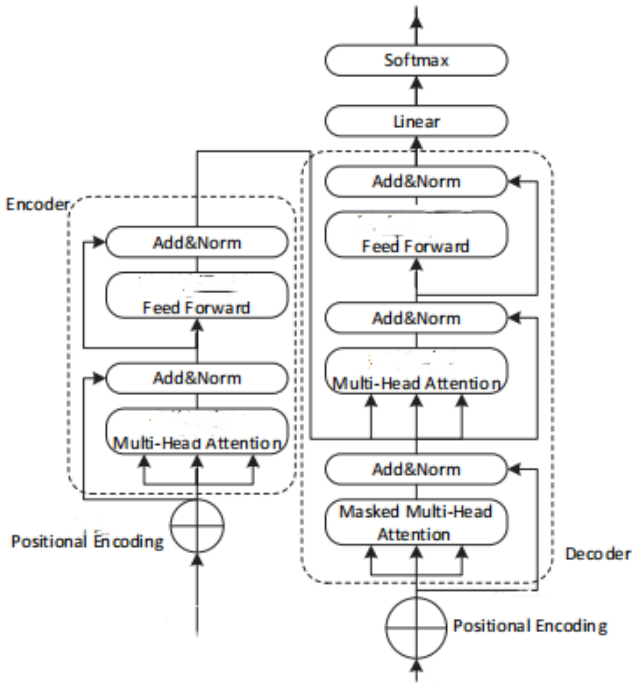


Figure 4. Transformer model structure

DOI: 10.54254/2755-2721/2026.KA26657

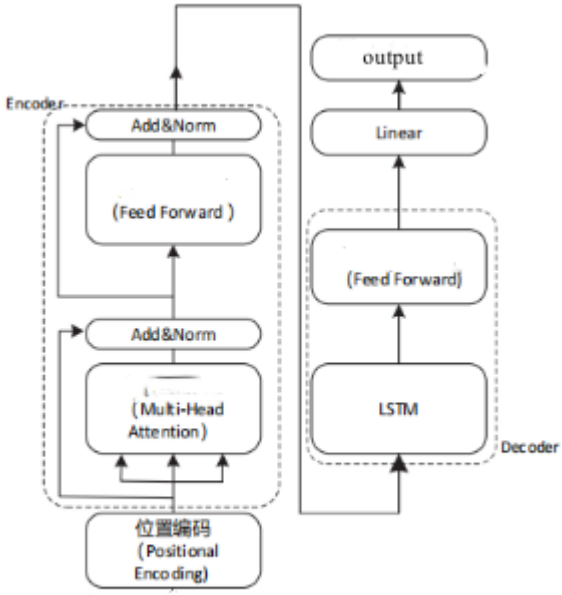


Figure 5. Transformer-LSTM

3. System integrator

3.1. Data sources

Taking 25000 tons bulk carrier as an example, the data source of the ship is divided into two ways, one way is to collect data in real time through the outboard environmental sensors, [4]and input the data into the Transformer-LSTM model after processing to generate the theoretical optimal carbon emission baseline value, as shown in Table 1; the other way is to set up the optimal operating parameter interval of the quadruple-supply device, and to realize real-time collection and transmission of operating data by relying on a series of networked and distributed high-precision sensor arrays and intelligent transmission units, as shown in Table 2. [5]The other way is to set the optimal operating parameter interval of the quadruple-supply device, relying on a series of networked distributed high-precision sensor arrays and intelligent transmission units to realize the real-time collection and transmission of operating data, as in Table 2.[6]

DOI: 10.54254/2755-2721/2026.KA26657

Table 1. Sensor selection for the first data channel

Sensor type	Sensor Model	measured variable	Measurement range
GPS sensor	Garmin GPS 18X HS	Longitude, latitude	0-180° (longitude), 0-9° (latitude)
Ship Speed Sensor	S518	ship's speed	0-30 sections
Rudder Angle Sensor	Koden KMC-170	helm angle	-180° to 180°
Wind Speed Sensor	Young 05103	air velocity	0-60 m/s
Water velocity sensors	RDI Workhorse	water velocity	0-3 m/s
Draught Depth Sensor	Aanderaa RCM 9	draft	0-20 meters
Wave Sensor	SubC Wave	Wave Significant Height	0-5 meters
temperature sensor	Omega 320-1	sea surface temperature	-20°C to 50°C
Carbon dioxide sensors	Aeroqual Ozone Series	Carbon dioxide concentration	0-5000 ppm
Buoy Sensor	Aanderaa 426	depth (of waterway)	0-30 meters

Table 2. Second Data Channel Sensor Selection

Crew Module	Sensor Name	model number	Range/Parameter
ORC two-stage generator sets	thermocouples	WRNK-431	0-450°C
Three-effect absorption heating and cooling units	Pressure Transmitter	Rosemount 3051S	0-60bar
	Solution Concentration Sensor	Anton Paar DMA 4500M	0-60wt% LiBr
	Pressure sensors	WIKA S-20	0-1500mmHg
Desalination unit	Salinity Monitor	HACH SL1000	0-50PSU
Energy Efficiency Management Platform	Temperature Acquisition Module	Niagara Tridium TAH201	PT100 input
	smart meter	Siemens 7KM2112	0-690V AC
Special Sensors	Efficiency Sensor Set	Fluke 2680A + Promass 83	Heat flow 0-2000W/m²

3.2. Construction of transformer-lstm-based multidimensional time series modeling

3.2.1. Preprocessing of data

The data in this study comes from Shanghai Maritime University Yuming ship internship bulk carrier, including the current ship's navigation status, marine environmental parameters and main engine and auxiliary engine energy consumption indexes of a total of 23 types of input data, so it is necessary to preprocess and construct a multi-dimensional time column input suitable for deep learning, such as Table 3.

DOI: 10.54254/2755-2721/2026.KA26657

Table 3. Data characterization and processing

feature category	Example of Input Data Containing Fields	Pre-processing methods
ship's condition	Speed, ROT, Draught	Z-score standardization
marine environment	Wind_Speed, mean_wave_period	Standardized + sliding average smoothing
Orientation parameters	Relative Wind Direction	Sine-cosine coding
geographic location	Lon, Lat	Original value retained
thermodynamic parameter	sea_surface_temperature	standardization

Equate the original date variable to hour, day_of_week, and month, and use sine-cosine coding to eliminate breakpoints with periodicity:

$$hour_sin = sin\left(2\pi * hour/24\right) \tag{5}$$

$$hour_cos = cos\left(2\pi * hour/24\right) \tag{6}$$

Z-score normalization of variable features such as Speed, Wind_Speed, and Draught:

$$x_{norm} = \frac{x-u}{\sigma} \tag{7}$$

Decompose the variables related to direction angle such as Relative Wind Direction and Relative Current Direction into two-dimensional vectors:

$$dir_x = cos\left(\theta\right) \tag{8}$$

$$dir_y = sin\left(\theta\right) \tag{9}$$

The raw values of Lon and Lat, which are geographic features, are retained directly for modeling regional differences in ocean conditions.

Outliers will be detected using a modified Hampel filter where MAD (Median Absolute Deviation) is defined as $median\left(\left|x_i - median\left(X\right)\right|\right)$,using linear interpolation instead of anomalous fluctuation values:

$$outlier = \left|x_i - median\left(X\right)\right| \geq 3 * MAD \tag{10}$$

3.2.2. Model architecture setup

In this paper, we innovatively propose Transformer-LSTM hybrid architecture on ships as in Figure. 6, which fuses global dependency modeling with local temporal pattern capturing capability.

DOI: 10.54254/2755-2721/2026.KA26657

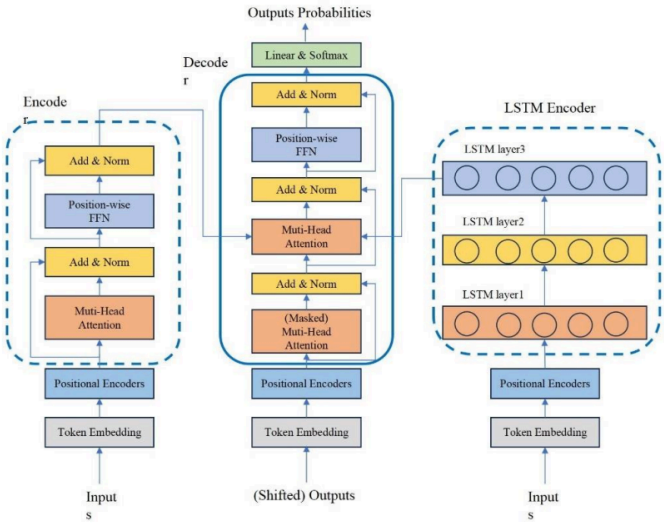


Figure 6. Transformer-LSTM modeling

①Input Layer:

Tensor dimension: $X \in R^{B*T*d}$,where B is the batch size, $T = 24$ is the synchronization duration, and $d = 23$ is the dimension feature.

②Transformer encoding module:

Multi-head self-attention mechanism: set up 8 attention heads, $d_k = d_v = d/8 \approx 23/8 \approx 3$

$$Attention\,(Q, K, V) = softmax\left(\frac{QK^T}{\sqrt{d_k}}\right)V \tag{11}$$

Positional coding: using a coding matrix capable of learning $P \in R^{T*d}$,summed with input features:

$$X^{'} = X + P \tag{12}$$

Layer with residual linking: the output of each layer is:

$$Layer\,(X) = LayerNorm\,(X + Dropout\,(FFN\,(Attention\,(X))))$$

where the FFN in the feedforward network contains two fully connected layers with dimensions from 265 to 23 and an activation function of GULU.

③LSTM timing modeling module:

Receive the context-enhanced sequence output by Transformer $H_{trans} \in R^{B*T*d}$, Extract timing features by two-layer LSTM:

$$h_t, c_t = LSTM\left(h_{t-1}, c_{t-1}, H_{trans}^t\right) \tag{13}$$

④ output layer:

where the hidden state will be mapped through the fully connected network CO2 predicted value:

DOI: 10.54254/2755-2721/2026.KA26657

$$\hat{y} = W_2 * ReLU\left(W_1 * h_T + b_1\right) + b_2 \tag{14}$$

among others $W_1 \in R^{128*64}$, $W_2 \in R^{64*1}$

3.2.3. Results of model predictions

Experimental results (Figure.7) demonstrate that the Transformer-LSTM hybrid model significantly outperforms the single LSTM model, reducing MAE and RMSE by 7.8% and 14.1% respectively ($p<0.05$), while MAPE decreased sharply from 136.3% to 57.0%,[7] indicating qualitative improvement in learning ship emission features. The R^2 increase from 0.12 to 0.33 validates the model's capability to analyze complex operational condition-carbon emission correlations. Technically, the Transformer's multi-head attention captures long-period features (e.g., speed, sea state) while LSTM gating maintains sensitivity to micro-dynamics (e.g., engine load), synergistically enabling multi-scale feature modeling.[8]This reduces single-voyage carbon emission errors by ~2.3 tons, significantly enhancing quadruple-supply system control accuracy and providing a credible data baseline for dynamic scheduling optimization.

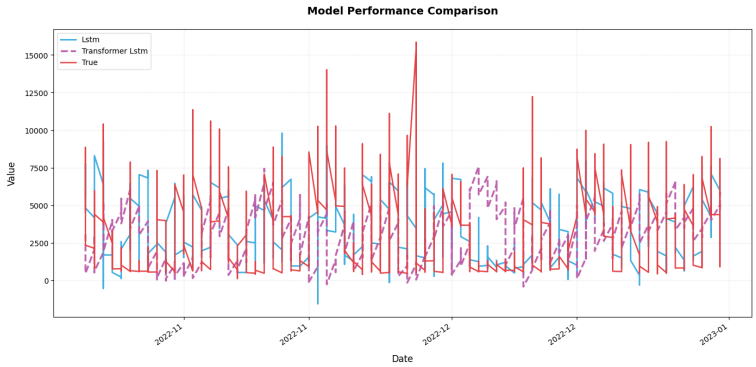


Figure 7. Comparison of different prediction models

3.3. Construction of dynamic scheduling algorithms for quadruple-supply

This project constructs an intelligent scheduling model for the quadruple-heating system (power generation, refrigeration, heating, seawater desalination) using a Python-based core framework. The model integrates multi-physical field parameters (e.g., flue gas temperature: 350-390°C, jacket water temperature: 90°C) and employs a multi-objective optimization architecture targeting emission reduction, energy efficiency, heat utilization, and freshwater production. Real-time calculation via a weight mapping dictionary generates Pareto-optimal solutions, trained using the Adam optimizer (1000 iterations, varied strategy ratios).[9]

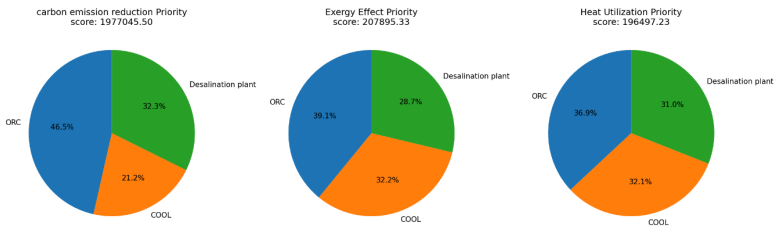


Figure 8. Scheduling adjustment effects

DOI: 10.54254/2755-2721/2026.KA26657

3.4. Summary of innovations

This study pioneers the integration of a Transformer-LSTM model with a quadruple-function waste heat recovery system for retrofitting aging ocean-going bulk carriers. The core innovation is a dual-channel intelligent synergy control architecture (Figure. 9).[10] The environmental regulation channel utilizes outboard sensors and the Transformer-LSTM model to dynamically generate an optimal carbon emission baseline, triggering actuator adjustments to the recovery system upon significant deviations. Concurrently, the process regulation channel employs high-precision internal sensors to monitor equipment performance and issue corrective commands during abnormal fluctuations.[7] This dual-loop mechanism synergistically links real-time environmental conditions with internal system responses, significantly enhancing dynamic regulation, stability. [11]

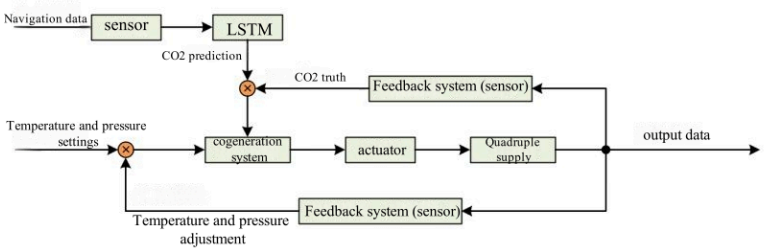


Figure 9. Automated control systems

4. Conclusion

The proposed dual-channel intelligent control framework, combining Transformer-LSTM-based carbon prediction with an advanced quadruple-supply waste heat system, represents a significant step forward in intelligent maritime energy management. This approach not only improves predictive accuracy and energy utilization under complex marine conditions, but also delivers a scalable, retrofittable pathway for legacy vessels to meet increasingly stringent decarbonization mandates.[12]

In the broader context, this integrated architecture addresses key bottlenecks in current maritime emission control—namely, the limited predictive capabilities of conventional models and the insufficient coordination across onboard energy systems.[13] By linking emission forecasting with dynamic system scheduling, the solution ensures consistent compliance with EEXI and CII standards while enhancing fuel economy and reducing greenhouse gas emissions.[14]

Looking ahead, the model holds substantial potential for expansion to other vessel types and energy management scenarios. Future research may further improve the robustness of the control logic under extreme sea states, explore fusion with renewable onboard energy sources,[15] and apply reinforcement learning to autonomously optimize decision-making over longer voyages. Ultimately, this work lays a technical foundation for achieving the IMO 2050 decarbonization goals through intelligent, data-driven ship operations.[16]

References

[1] HUANG Jinjie, JIANG Zhaoming, LU Junbing. Response to EEDI, EEXI and CII indices [J]. Navigation, 2023(2): 58-64.

[2] ZHAO Hai-Li, LI Shan-Wen, ZHANG Dat-Tian, et al. Case study of silicone antifouling paint Hempaguard on real ships EEXI and CII [J]. Modern Coatings and Painting, 2025, 28(1): 21-23+40.

DOI: 10.54254/2755-2721/2026.KA26657

[3] GUI Binglin, LIU Chunyu, LIU Jiapeng. Multifactor carbon emissions trading price prediction based on Transformer-LSTM model [J]. Price Monthly, 2024, (5): 49-57.DOI: 10.14076/j.issn.1006-2025.2024.05.06.
[4] Chen, Zhongdu, Xu, Chunchun, Ji, Long, et al.Carbon footprint analysis of double cropping rice production in the middle Yangtze River Valley based on household surveys [J].Chinese Journal of Rice Science, 2018, 32(6): 601-609.DOI: 10.16819/j.1001-7216.2018.7080.
[5] HsiaoHwa Chen, Yi Qian, Sheng Zhou.ENERGY CONSERVATION AND HARVESTING FOR GREEN COMMUNICATIONS [J].China Communications, 2014, 11(3): I0001-I0002.
[6] Ma Li.A Greener Path [J].Beijing Review, 2016, 59(18): 36-37.
[7] MOST Developed Software of Counter of Energy Conservation and Emission Reduction for Public [J].Chinese Journal of Population, Resources and Environment, 2008, 6(2): F0003-F0003.
[8] Li, Zhengze, Chen, Xuan, She, Anming, et al.Adjusting LCA Allocation Methods for Cement Industry: A Production-Based Approach to Energy Conservation and Emission Reduction [J].MATERIALS, 2025, 18(11).DOI: 10.3390/ma18112483.
[9] Berselli, Luigi C., Chiodaroli, Elisabetta, Sannipoli, Rossano.Energy Conservation for 3D Euler and Navier-Stokes Equations in a Bounded Domain: Applications to Beltrami Flows [J].JOURNAL OF NONLINEAR SCIENCE, 2025, 35(1).DOI: 10.1007/s00332-024-10102-x.
[10] Sun, Mulin, Fu, Yuhao, Sun, Mingyao, et al.Study on Key Influencing Factors of Carbon Emissions from Farmland Resource Utilization in Northeast China Under the Background of Energy Conservation and Emission Reduction [J].ENERGIES, 2025, 18(2).DOI: 10.3390/en18020277.
[11] Wang, Chun-Chun, Wang, Yuan, Zhu & Xiao-Dong.(2019).Peak volume and time of energy-related CO2 emissions in Jiangsu Province, China based on long-range energy alternatives planning system model.Ying yong sheng tai xue bao = The journal of applied ecology, 30(10), 3535-3543.DOI: 10.13287/j.1001-9332.201910.017.
[12] Suo, Liang, Li, Shugang, Wu, Fengliang, et al.The Effect of Distance between Jet Fans on Gas Transport, Energy Conservation, and Emission Reduction in Long Highway Tunnels [J].SUSTAINABILITY, 2024, 16(16).DOI: 10.3390/su16166990.
[13] Xu, Xingshuo, Zhou, Chang, Tan, Yansi, et al.Analyzing the Diversion Effect of Debris Flow in Cross Channels Utilizing Two-Phase Flow Theory and the Principle of Energy Conservation [J].WATER, 2024, 16(15).DOI: 10.3390/w16152134.
[14] Harini, R., Indhira, K..Dynamical modelling and cost optimization of a 5G base station for energy conservation using feedback retrial queue with sleeping strategy [J].TELECOMMUNICATION SYSTEMS, 2024, 86(4): 661-690.DOI: 10.1007/s11235-024-01155-0.
[15] Zhang, Yingbin, Li, Xiaoqin, Fu, Junwen, et al.Quick analysis model for earthquake-induced landslide movement based on energy conservation [J].LANDSLIDES, 2024, 21(6): 1315-1331.DOI: 10.1007/s10346-024-02223-x.
[16] Conte, Dajana, and FrascaCaccia, Gianluca."Exponentially fitted methods with a local energy conservation law." ADVANCES IN COMPUTATIONAL MATHEMATICS 49.04(2023).DOI: 10.1007/s10444-023-10049-9.